Coupling particles and fields in a diffusive hybrid model

E. G. Flekkøy,[1,2] J. Feder,[1,2] and G. Wagner[3]
[1]*Department of Physics, University of Oslo, PB 1048 Blindern, 0316 Oslo, Norway*
[2]*Fracton as, Tåsenveien 74C, 0873 Oslo, Norway*
[3]*School of Astronomy and Physics, Raymond and Beverly Sackler Faculty of Exact Sciences, Tel Aviv University, Ramat Aviv, 69978 Tel Aviv, Israel*
(Received 2 January 2001; revised manuscript received 2 July 2001; published 14 November 2001)

A general scheme to patch together discrete and continuous descriptions of diffusion within the same physical space is studied. In the discrete description, diffusion is described by microscopic random walkers on a lattice; in the continuous description, diffusion is described through the macroscopic diffusion equation. The coupling scheme is based on the mutual exchange of mass flux across the discrete-continuous interface. Detailed tests of the scheme, coupling particle, and field descriptions are particularly illustrative for the diffusion problem. Both the nonequilibrium transport behavior and the equilibrium fluctuations of the combined discrete-continuous system are in agreement with theoretical predictions.

DOI: 10.1103/PhysRevE.64.066302 PACS number(s): 47.11.+j

I. INTRODUCTION

The diffusion equation is at the heart of so many physical descriptions that it is hard to list them all. Physical quantities such as heat in a solid, momentum in a fluid, or a pollutant in a gas may all be described by the diffusion equation. The same can be said for the probability of finding a grain of pollen undergoing Brownian motion in space. In fact, all types of random microscopic motion with a finite step length and a finite correlation time satisfy the diffusion equation in the macroscopic limit. In that limit, i.e., on spatial scales larger than the correlation length of the underlying microscopic processes, one may expand the current of the relevant quantity in a series of the density gradient of the same quantity to obtain Fick's law. Then the diffusion equation follows as a statement of conservation of the quantity at hand.

It is precisely when the physical processes produce a structure at the scale of the microscopic correlation length that one runs into trouble with the diffusion equation. In this case there might not exist a simple macroscopic description, and if it does, it will not be linear in the density gradient. For concreteness one may think of the heat transport around a fracture formed within a solid under stress. Here a heat source (the propagating fracture) is localized over a few atomic lengths, and thus is singular on the macroscale. While the diffusion equation in this case may still describe the large-scale transport of heat, it does not describe the pattern of local transport. Local heat flow may, however, influence the further growth of the fracture, and thus be of interest.

Indeed, there exist processes on macroscopic length scales that, for fundamental reasons, cannot be described by continuum theory; they must be treated on the discrete atomistic scale. Famous examples of such processes include the moving contact line between two immiscible liquids moving on a substrate [1], the breakup and merging of fluid droplets [2], strong shear localization, dynamic melting processes [3], and the evolution of a fracture tip [4–6]. For a modeling of such processes it is of fundamental interest to combine a local and detailed particle description with a continuous field description of greater numerical economy. In this paper we introduce a simple coupling scheme for this purpose in the case of diffusion. It represents a highly simplified version of the hydrodynamic coupling scheme introduced in Ref. [7]. Contrary to existing coupling schemes [8–10], the present scheme and that in Ref. [7], are based entirely on the exchange of *fluxes*, which is the most direct and general way to enforce the pertinent conservation laws.

Diffusive processes may require atomistic or discrete descriptions in cases where fluctuations are important, such as in small scale deposition-dissolution processes or when gradients become large and Fick's law breaks down. More generally, fluctuations arise naturally whenever a particle description is required. However, in existing continuum-particle hybrid models [8–10], the focus is on the *average* behavior. The main virtue of the present paper is an analysis of the fluctuations. The leading question is to what extent the continuum acts as a statistical mechanical reservoir for the particle system. We quantify the answer to this question by means of both analytical arguments and measurements, and we demonstrate that the agreement between the two is reasonable. The main result is that, depending on the coupling to the continuum, the size of the particle fluctuations interpolates between those of an open system and those of a closed system. However, in order to make an analysis of the *fluctuating* behavior of the model meaningful, we first check that it has the correct *average* behavior. This is done in a sequence of simple test cases in the beginning of the paper.

Interestingly, hybrid descriptions may also be useful in the opposite application where particles are used in the low resolution region and a continuum description is used where high resolution is required. This is the case in a recent work by Plapp and Karma [11], who studied dendritic growth on scales where fluctuations are not considered. The coupling scheme used in this study derives the particle boundary condition from the continuum flux, whereas the continuum boundary condition is derived from the particle *density*. Hence flux continuity is not obvious from this scheme.

Particle models that seek to bridge the gap between microscopic and macroscopic scales do exist—most notably the hydrodynamic models known as dissipative particle dynam-

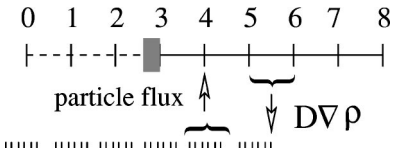

FIG. 1. Sketch of the coupling scheme of the hybrid model in the special case where there are nine sites on the continuum lattice and $W=6$ particle sites per continuum site. The particle system (P) is coupled to the continuum (C) at the location of the right arrow, and the continuum to the particles at the left arrow.

ics [12,13]. Even though these models have recently evolved to include an adaptive range of particle scales [14,15], they remain mesoscopic in the sense that their particles are coarse grained representatives of the underlying microdynamics.

II. MODEL

To describe a diffusive process on a microscopic scale, we consider a set of random walkers moving on the sites of a one-dimensional lattice. The random walkers move with equal probability to the left or the right, hopping from one site to a neighboring site during each time step. This discrete, microscopic description is coupled to a continuous, macroscopic description, obtained by solving a discretized version of the diffusion equation

$$\frac{\partial \rho_c}{\partial t} = D\nabla^2 \rho_c \tag{1}$$

on a one-dimensional array of nodes. Here ρ_c is the density of random walkers or particles on a continuum node, and D is the macroscopic diffusion constant. The two descriptions overlap to some extent, in the sense that some of the continuum nodes and some sites of the particle lattice cover the same region of space. This is shown in Fig. 1. One continuum node corresponds to $W>1$ lattice sites of unit length on which the particles move. As units we shall take the lattice constant of the particle lattice and the time step of the particles, i.e., every particle moves a unit length in a unit time. The lattice constant of the continuum lattice (on which we discretize the diffusion equation) is therefore W, which is the number of particle step lengths per continuum node. The density ρ_c is defined on the continuum nodes, and the particle density ρ_p is the number of particles per site on the more fine grained lattice. In equilibrium the averages of ρ_p and ρ_c will be equal.

The general idea of particle-continuum hybrid models is to resolve finer space and time scales in the particle system than in the continuum, which thus is taken to represent a coarse grained description of the particle system. One time step in the iteration of Eq. (1) thus corresponds to τ microscopic time steps. Since particle time steps are taken to have a unit length, the time step of Eq. (1) is simply τ. In fact a main virtue of the coupling scheme is that it allows this separation of both the space and time scales of the two domains.

Since the particle system has intrinsic fluctuations it would appear that one would need to add a fluctuating term to the above diffusion equation to obtain a fully consistent picture. It is clearly possible to do this along the lines of fluctuating hydrodynamics [18]. However, the main effect of the continuum on the particle number fluctuations is linked to the averaging of the particles that is needed in the coupling region. Moreover, the general idea is to link a fine scale description (the particles) to a region of coarser scale where fluctuations in general play a less important role. This was the view taken in previous studies

The basic idea of the coupling scheme is to impose the flux of the particle system as a boundary condition on the continuum at one location, and to do the reverse at another location. This is illustrated in a particular case in Fig. 1, where an overlap zone is defined between sites 4 and 6. At site 4 the particle flux is imposed on the continuum, and at the rightmost site on the particle system the flux of the continuum system is imposed on the particle system. Sites 0–3 are represented by the particle system only, and the continuum equation is not updated there.

Figure 1 shows where these fluxes are imposed. The mass flux $D\nabla\rho$ in the continuum, where $\nabla\rho$ is evaluated from sites 5 and 6, is imposed as a source term on the second outermost site of the particle lattice (at the outermost site which is not shown the particles just bounce back to the left).

Once the continuum flux is computed it is imposed as a particle source which is constant over the τ particle updates. Then, at the last of these updates, the particle flux j_p is averaged over W sites, and used to define the source on the continuum. More precisely, $D\nabla\rho_c$ particles are added to the particle system every update. In doing this, $D\nabla\rho_c$ is rounded to the closest integer.

Correspondingly, the continuum receives a mass $j_p\tau$ by adding this value at ρ_c at the site of the leftmost arrow of Fig. 1, i.e., site 4. The particle flux j_p is measured simply as the number of right moving particles minus the number of left moving particles at the given time.

Of course, the flux boundary condition on the continuum could also have been imposed as a condition on the concentration gradient. However, since this condition represents a noise source that imposes variations on all wavelengths down to the lattice scale, it does not conserve mass (the integrated concentration) to a high accuracy. This was checked in independent simulations using the continuum equation solver and a random boundary condition. In these simulations the imposition of a source term conserves mass to a higher accuracy than the imposition of a concentration gradient.

As usual in the numerical treatment of differential equations, the gradient of the density must be expressed as a difference across nodes. In particular, to express the continuum flux density the difference gradient

$$\nabla\rho_c \approx \frac{\rho_c(x_6)-\rho_c(x_5)}{W}, \tag{2}$$

where x_5 and x_6 are shown in the figure, should be used. Note that since the site of the particle source is located right between x_5 and x_6 the difference expression above is really a

centered difference. The discrete value of $\nabla\rho_c$ then defines the flux density at the boundary of the continuous domain.

However, Eq. (2) does not prevent discontinuities at the discrete-continuous interface. Indeed, a configuration with $\rho_p = \text{const}$ everywhere in the discrete domain, and $\rho_c = \text{const}$ everywhere in the continuous domain, would lead to vanishing averaged fluxes, even for $\rho_p \neq \rho_c$. Equilibration is enforced if a hybrid gradient ∇' of the form

$$\nabla'\rho_c \approx \frac{\rho_c(x_6) - \rho_p(x_5)}{W} \tag{3}$$

is employed to define the flux $D\nabla\rho_c$ into the particle system. In Eq. (3), the macroscopic continuum density is *replaced* by the corresponding microscopic density characterizing the node x_5. The imposed flux of random walkers, based on Eq. (3), enforces that, on average, $\rho_p = \rho_c$ at the discrete-continuous interface. When the coupling scheme is applied to a physical system involving both mass and momentum transport [7], one may do without this device and use Eq. (2), as density mismatch at the interface will lead to momentum and mass flux exchange and equilibration by default.

As an illustration of the fact that continuum descriptions generally capture only the large scale behavior of the particle system, note that the average particle evolution is not exactly described by Eq. (1). Equation (1) only contains the lowest order in the gradient terms. In fact, it is generally possible—for instance by applying a simple version of the standard Chapman-Enskog expansion technique [16,17]—to show that the diffusion equation contains correction terms of higher order in ∇^2, that become important when density gradients are large. When gradients are small on the lattice scale, or the scale of the mean free path, Fick's law is generally valid to an excellent approximation.

III. SIMULATIONS AND RESULTS

The simulations focus on two main questions. (i) Is the time-dependent mass transport across the discrete-continuous interface continuous and smooth? (ii) In what sense does the continuum domain represent a continued thermodynamic bath for the discrete system of random walkers?

If not stated otherwise, $W = 20$ lattice sites were taken to correspond to one continuum node, and between five and 20 random walkers were employed per lattice site. The continuum description was evolved by means of a Cranck-Nicholson finite difference scheme, using the diffusion constant $D = 0.5$ lattice constant^2/time step. D is then equal to the diffusivity of a single random walker.

A. Transport properties and the continuity of the discrete-continuous interface

Is the coupling mechanism able to propagate the diffusive current continuously across the discrete-continuous interface? Figure 2 shows results from simulations intended to test the transport properties of the hybrid model. A discrete domain containing 210 sites was patched together with a continuum extending on 33 nodes, also counting the leftmost sites that are not updated. The continuum time step was set to

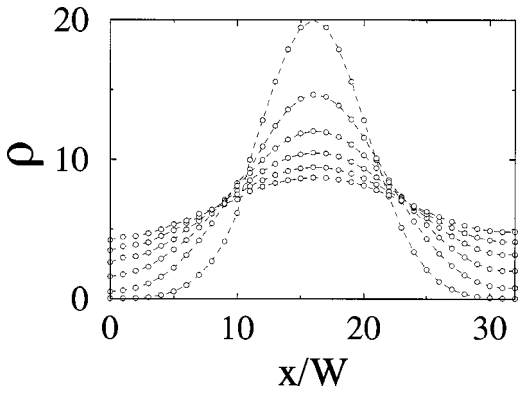

FIG. 2. A relaxing Gaussian density profile in a one-dimensional box of size $32W$, shown at six different times $t = 0$, 6, 12, 18, 24, and 30×10^3 particle time steps. The particle domain covers the leftmost $x/W \leqslant 10$ positions. The data were averaged over 100 independent runs, and the particle density data were averaged over a space of W sites at each node position.

$\tau = 50$ (in units of microscopic time steps), and each run was over 30.000 particle time steps. A Gaussian density profile was imposed initially, and left to relax. Averaging over an ensemble of 100 independent runs, the density profile runs continuously across the discrete-continuous interface, and the microscopic fluctuations in the discrete domain are barely visible. Note that the microscopic densities of every W sites were averaged to yield one data point, corresponding to one node position.

Figure 3 shows the same data as Fig. 2 but only the difference $\Delta\rho(x/W) = \rho(x/W) - \rho(32 - x/W)$. Each run conserved total mass within 0.5%. The main particle-continuum discontinuity is present in the initial configuration. The particle system was initialized with steps of width W and constant density.

For comparison with the case where mass flows out of, and not into, the particle system, Fig. 4 shows density profiles measured during a single run, using the same combined discrete-continuous system. Two Gaussian profiles, centered at the extreme ends of the domains, were imposed initially and left to relax. Here the microscopic fluctuations are

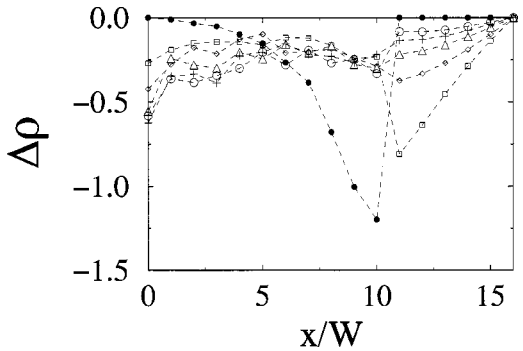

FIG. 3. The difference $\Delta\rho(x/W) = \rho(x/W) - \rho(32 - x/W)$ as a function of x, where $\rho(x)$ is shown in Fig. 2. The sequence of symbols ●, □, ◇, △, +, and ○ corresponds to the time sequence $t = 0$, 6, 12, 18, 24, and 30×10^3 particle time steps.

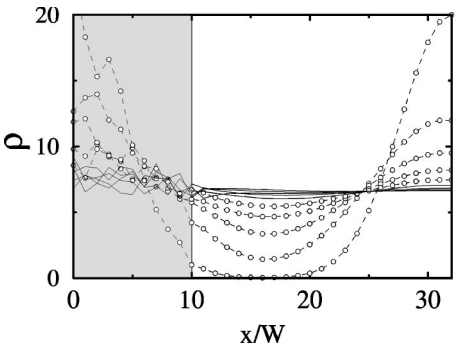

FIG. 4. Two relaxing Gaussian density profiles in a one-dimensional box, shown at various stages. The same system and plot scale as in Fig. 2 were used, and the discrete domain is indicated by the shaded area. The microscopic density data were averaged over a space of W sites at each node position.

clearly visible, in sharp contrast to the smooth profile obtained in the continuous domain.

In the simulations illustrated in Figs. 2 and 4, the initial state was symmetric around the center of the hybrid system, and the extreme end boundary conditions were reflective. Hence density profiles, which initially were symmetric in space, should preserve symmetry. The coupling scheme may be tested by directly comparing the left- and right-hand portions of the graph. These were indeed found to evolve symmetrically, up to the effect of microscopic fluctuations. As an independent check, it was verified that the microscopic density profile of random walkers alone indeed evolved with a diffusivity of $D=0.5$.

In another independent test of the coupling scheme in the more realistic case of source terms present, random walkers were injected at the left hand side of the combined discrete-continuous system, starting from $\rho_p=\rho_c=0$ everywhere. Figure 5 shows the resulting density profiles, obtained by injecting one walker every 20 microscopic time steps, and averaging the profiles from ten independent runs.

In this, as in former cases, analytical results are readily available. Let us denote the source by s, which is the number

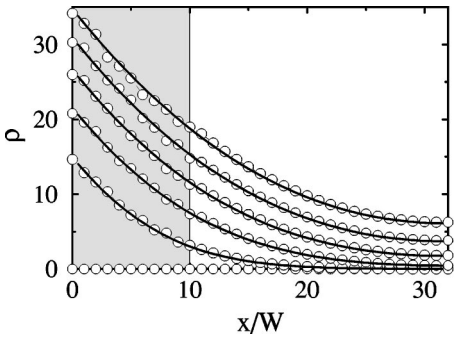

FIG. 5. Increasing density profiles in a one-dimensional box. The same system and plot scale as in Fig. 2 were used, and the discrete domain is indicated by the shaded area. Random walkers were slowly fed from the left, starting with zero density everywhere. Circles indicate the results of the hybrid simulation, averaged over ten independent runs, and solid lines show the theoretical prediction given in Eq. (5). The microscopic density data were averaged over a space of W sites at each node position.

of injected particles per time step at the leftmost node position (s may be less than 1). Equation (1) then takes the form

$$\frac{\partial\rho}{\partial t}=D\nabla^2\rho+2s(t)\,\delta(x), \tag{4}$$

where δ is the Dirac δ function, and the factor 2 is due to the reflecting boundary condition at $x=0$ (in the open-space scenario described by the diffusion equation, half the particles escape to the left, in contrast to the simulated scenario). Using the Green's function of the diffusion equation, the solution to Eq. (4) is easily written down as

$$\rho(x,t)=\int_0^t dt'\frac{1}{\sqrt{4\pi Dt'}}\exp\left(\frac{-x^2}{4Dt'}\right)2s(t'). \tag{5}$$

This expression was evaluated numerically to give the solid lines in Fig. 5. We note that in this figure the diffusion equation is simultaneously solved in three different ways, and the agreement between the results is seen to be good.

Switching off the source, it was found that the density profile relaxed to a constant value everywhere in the hybrid system. In the final state the fluctuations in the discrete domain, were seen to propagate into the continuous domain, where they damped out as they progressed rightward.

B. Equilibrium fluctuations

In what sense does the continuum define a thermodynamic reservoir for the discrete system of random walkers? Ideally, the continuum should behave as an extended particle system. However, in contrast to an extended particle system, the continuum density does not fluctuate on microscopic time and length scales. While it would be possible to add fluctuations to the continuum along the lines of *fluctuating hydrodynamics* [18], in the following we will study the coupling to the fluctuationless continuum.

The coupling scheme is characterized by two parameters: the ratio W of macroscopic to microscopic length scales, and the ratio τ of macroscopic to microscopic time scales. We shall examine how the particle number fluctuations depend on W and τ. The particle flux density j_p that is imposed on the continuum in the $P\rightarrow C$ region is given by the sum of the particle currents J_i that characterize each of the W sites in the underlying microscopic lattice,

$$j_p=\frac{1}{W}\sum_{i=1}^{W}\overline{J_i}=\frac{\overline{J}}{W}, \tag{6}$$

where the line denotes time averaging over τ microscopic time steps. The instantaneous net current across the $P\rightarrow C$ region is $J=R-L$, where R and L is the total number of right- and left-moving random walkers, respectively, in the region, and J_i is the corresponding quantity on particle site i.

Since the particle number fluctuations are a result of the fluctuations in j_p, we need to compute $\overline{\langle j_p^2\rangle}$, where the brackets $\langle\cdots\rangle$ denote an ensemble average. First we evaluate $\langle J^2\rangle$ in the equilibrium state when $\langle J\rangle=0$. Denoting the

particle number in the $P \rightarrow C$ region by $N_W = R + L$, and making use of $\langle R \rangle = \langle N_W \rangle / 2$, we can compute $\langle J^2 \rangle$ as

$$\langle J^2 \rangle = \langle R^2 - 2RL + L^2 \rangle = \langle 4R^2 - N_W^2 \rangle$$
$$= \sum_{N_W=0}^{\infty} Q(N_W) \sum_{R=0}^{N_W} P_N(R)(4R^2 - N^2), \qquad (7)$$

where the probability of finding N_W random walkers in the $P \rightarrow C$ region is given by the Poisson distribution

$$Q(N_W) = \frac{e^{-\langle N_W \rangle} \langle N_W \rangle^{N_W}}{N_W!}, \qquad (8)$$

and the probability that R of these N_W random walkers are moving right is given by the distribution

$$P_{N_W}(R) = \frac{1}{2^{N_W}} \binom{N_W}{R}, \qquad (9)$$

where

$$\binom{N_W}{R} = \frac{R!}{N_W!(N_W - R)!} \qquad (10)$$

is the binomial coefficient. We may then compute the current fluctuation

$$\langle J^2 \rangle = \sum_{N_W=0}^{\infty} Q(N_W) \sum_{R=0}^{N_W} P_{N_W}(R)(4R^2 - N_W^2)$$
$$= \sum_{N_W=0}^{\infty} Q(N_W) N_W = \langle N_W \rangle. \qquad (11)$$

It may be noted from the last equality that the same result for $\langle J^2 \rangle$ would have been obtained if we had assumed a fixed particle number $\langle N_W \rangle$, and computed the fluctuations due to the flipping between right and left moving particles only. In other words, the microcanonical and grand canonical ensembles produce the same current fluctuations. Now, in order to obtain the fluctuations in the averaged current according to Eq. (6), we need to carry out a time average as well. But this is an easy task since there is no difference between the independent events that occur over time and those that occur over space. If in Eq. (11) the average is also taken over a time span τ, we only need to replace the number N_W of particles by $N_W \tau$. Since a time average of the current J implies the division by a factor τ, the total result of the averaging is, with Eq. (6),

$$\langle j_p^2 \rangle = \frac{\langle N_W \rangle}{\tau W^2} = \frac{\rho_p}{\tau W}. \qquad (12)$$

We now assume that the continuum is transmitting the fluctuations imposed on its boundary region without damping or distortion to the $C \rightarrow P$ region, where the boundary flux of microscopic random walkers is imposed. Indeed, the diffusive current that enters the continuous domain at $P \rightarrow C$ must create a corresponding flux further to the right. However, the coarse nature of the continuum description is likely to cause incorrect estimates of this current, since the imposed fluctuations cause relatively large density variations among adjacent continuum nodes; this in turn leads to poor approximations for the flux derivatives. This discretization effect is viewed as the main source of discrepancies in what follows. The ensemble-averaged fluctuations of the number of random walkers, in response to the imposed boundary conditions, are given by the particle densities as

$$\langle \delta N_W^2 \rangle = \int_V dx dx' \langle \delta \rho_p(x,t) \delta \rho_p(x',t) \rangle; \qquad (13)$$

the integrals run over the discrete domain of volume V, and $\delta \rho_p$ denotes the continuum-induced deviation of the particle density ρ_p from its mean value. To study the effect of fluctuations in the $C \rightarrow P$ region, the current density j_p imposed by the fluctuating continuum is included in the coarse-grained description of the discrete domain:

$$\partial_t \rho_p(x,t) = \nabla \cdot [D \nabla \rho_p(x,t) + j(x,t)]. \qquad (14)$$

Here ρ_p is the number of particles per particle site, and j is the imposed current which is assumed to obey the same statistics as the averaged microscopic current j_p. However, we now need its full correlations $\langle j_c(x,t) j_c(x',0) \rangle$. Clearly there are no equilibrium space correlations. Time correlations, however, are caused by the numerical scheme, since j_c does not change for τ microscopic time steps. As a result of this invariance and of Eq. (12), we obtain

$$\langle j(x,t) j(x',0) \rangle = \frac{\rho}{\tau} \sum_{i=1}^{\tau} \delta(t - t_i) \delta(x - x'), \qquad (15)$$

where t_i runs through integers from 1 to τ. Equations (14) and (15) are fully analogous to corresponding equations of the theory of fluctuating hydrodynamics. From a theoretical viewpoint it is interesting to note that it is possible to arrive at Eq. (15) by considering the entropy production associated with the entropy $S = -\int dx \rho(x) \log \rho(x)$ to identify the thermodynamic fluxes and forces. From this result a fluctuation-dissipation theorem that coincides with Eq. (15) may be derived.

Equation (14) may be solved by the introduction of the Fourier transforms,

$$j_k(t) = \frac{1}{V} \int dx j(x,t) e^{-ikx},$$

$$j(x,t) = \sum_k j_k(t) e^{ikx}, \qquad (16)$$

where $\int dx e^{i(k-k')x} = V \delta_{kk'}$, and V denotes the volume of the discrete domain.

Upon the application of this transform, Eq. (14) takes the form

$$\partial_t \rho_k = -k^2 D \rho_k + ikj_k, \tag{17}$$

which is easily solved to give

$$\rho_k(t) = ik \int_{-\infty}^{t} dt' j_k(t') e^{-k^2 D(t-t')}. \tag{18}$$

The Fourier transform of Eq. (15) gives

$$\langle j_k(t) j_{k'}^*(0) \rangle = \frac{\rho}{WV} \delta_{kk'} \frac{1}{\tau} \sum_{i=1}^{\tau} \delta(t - t_i). \tag{19}$$

Equation (13) may now be solved by the combination of Eqs. (16), (18), and (19). This gives the somewhat involved expression

$$\langle \delta N^2 \rangle = \int dx dx' \sum_{kk'} \int_{-\infty}^{t} dt' \int_{-\infty}^{t} dt'' k^2 \langle j_k(t) j_{k'}^*(0) \rangle \times \exp[-k^2 D(2t - t' - t'') + i(kx - k'x')]. \tag{20}$$

Using Eq. (19) we obtain

$$\langle \delta N^2 \rangle = \frac{\rho}{WV} \int dx dx' \sum_{k} \frac{1}{\tau} \sum_{i=1}^{\tau} \int_{-\infty}^{t} dt' \times k^2 \exp[-2k^2 D(t - t' + t_i) + ik(x - x')], \tag{21}$$

which upon time integration becomes

$$\langle \delta N^2 \rangle = \frac{\rho}{2DWV} \int dx dx' \sum_{k} \frac{1}{\tau} \sum_{i=1}^{\tau} \times \exp[-2k^2 D t_i + ik(x - x')]. \tag{22}$$

The integrals over x and x' are easily carried out. They give

$$\langle \delta N^2 \rangle = \frac{\rho_p V}{2DW} \sum_{k} \delta_{k0} \frac{1}{\tau} \sum_{i=1}^{\tau} e^{-2k^2 D t_i} = \frac{N}{W}, \tag{23}$$

where in the last step we used $D = 1/2$, $N = \rho_p V$, and $(1/\tau)\Sigma_{i=1}^{\tau} 1 = 1$. Note that since in the end only the $k = 0$ contribution was projected out by the x integration, $\langle \delta N^2 \rangle$ does not depend on the averaging time τ. Physically this is because the reduction in the current fluctuations, due to time averaging, is exactly balanced by the increased correlation time of the fluctuating current.

The above formalism could easily be extended to deal with space-time correlations of the density. However, these correlations will depend strongly on the underlying conservation laws in the system—in the present case, mass conservation only. For this reason these will be of less interest for a comparison with hydrodynamic systems [7], in which momentum is also conserved. The result of Eq. (23) is expected to be robust under changes of the dynamical rules.

It is of interest to note that in the $W \to 1$ limit Eq. (23) reduces to $\langle \delta N^2 \rangle = N$, which is the fluctuation of a system in touch with a real particle reservoir. This statistical mechanical result follows from the Poisson distribution of Eq. (8).

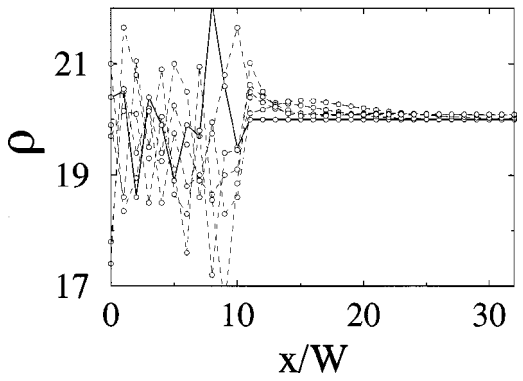

FIG. 6. The density profiles in the left half of the system measured at the different times $t = 0$, 2, 4, 6, 8, and 10×10^4 particle time steps. Here $W = 20$ $\tau = 10$, and the solid line shows the initial state.

In order to compare predictions and measurements, a sequence of equilibrium simulations with a flat initial density profile was carried out for different ratios W of macroscopic to microscopic length scales. The hybrid system parameters were the same as those used in Sec. II, except that the particle system only occupied 1/8 of an entire system of width $65W$. Conservation of the total mass M_{tot} only holds to within 1% in these simulations. The measurements of the fluctuations were corrected for this drift by measuring the deviations in particle number from the instantaneous value rather than initial value of $M_{tot}/8$. However, as is noted below, the drift still seems to have an effect. In Fig. 6 the density is shown at 5 consecutive stages. As before ρ is obtained from the particle data at $x/W \leqslant 10$. Note how the fluctuations are damped in the continuum part of the system. Care was taken so that the fluctuations did not significantly affect the right edge of the continuum $x/W = 64$, thus creating unwanted finite-size effects.

Figure 7 shows the fluctuations for different W values on a log-log scale. The fluctuations where ensemble averaged over 100 independent runs using $\tau = 10$. The prediction [Eq. (23)] gives $\log(\langle \delta N^2 \rangle / N) = -\log W$. The gray dashed line shows Eq. (23) with a correction term added to it, i.e.,

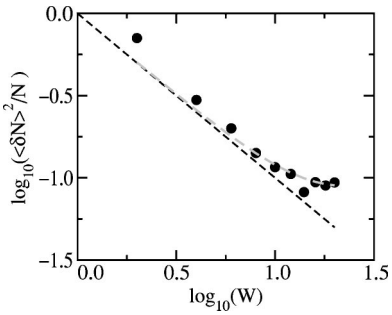

FIG. 7. The particle number fluctuation as a function of the number W of particle sites per continuum node. The black dashed line shows the theoretical result of Eq. (23), and the gray dashed line the result of Eq. (24).

$$\langle \delta N^2 \rangle = \frac{N}{W} + \alpha N^2, \tag{24}$$

with $\alpha = 10^{-5}$. While the main trend of the data in Fig. 7 is to confirm the theoretical prediction, the discrepancies between the measurements of Fig. 7 and the theory of Eq. (23) occur at small and large W, and to a lesser extent at intermediate values.

The theory assumes that particle and continuum fluxes coincide for all wavelengths and frequencies. This assumption is expected to work better when W is large and some of the rapid, short wavelength behavior of the particle system is averaged away. This may explain the small W departure between theory and measurement. At $W=1$ the noise level of the continuum boundary condition made the Cranck-Nicholson solver unstable. Hence $W=2$ is the smallest value shown.

Only the integer part of the flux $D\nabla\rho$ is imposed on the particle system. This error source is likely to be visible at all W, and most so when W is large. For the largest W it also appears that the small drift in particle number has an effect. Assuming that the drift in N is proportional to N, we obtain an N^2 contribution to δN^2 which is given in Eq. (24). This equation seems to give a good fit to the large W data, indicating that the crossover behavior at $W=14$ is due to the imperfect mass conservation.

IV. CONCLUSIONS

In principle, the presented coupling scheme can be applied to any pair of particle and field descriptions, in any dimension. Here we have studied both the equilibrium and nonequilibrium behaviors of a one-dimensional diffusive hybrid system. The coupling worked well after the introduction of a particle based modification for the computation of the continuum density gradient in the overlap region.

The nonequilibrium behavior, which is globally described by the diffusion equation, agreed well both with consistency checks and analytical predictions. In the equilibrium case we studied the particle fluctuations in order to establish the extent to which the continuous domain played the role of a well defined thermodynamic reservoir. It was found theoretically, and partly confirmed by simulations, that the role of the continuum approximates the role of a thermodynamic reservoir in the small W limit, while it completely suppresses fluctuations in the large W limit.

ACKNOWLEDGMENTS

G.W. was partially supported by Tel Aviv University and by Schweizerischer Nationalfonds. This research was also supported by the research contract 462000-98/0 between Norsk Hydro ASA and Fracton as.

[1] J. Koplik and J.R. Banavar, Annu. Rev. Fluid Mech. **27**, 257 (1995).
[2] M.P. Brenner, X.D. Shi, and S.R. Nagel, Phys. Rev. Lett. **73**, 3391 (1994).
[3] P.A. Thompson and M.O. Robbins, Science **250**, 792 (1990).
[4] F.F. Abraham, J.Q. Broughton, N. Bernstein, and E. Kaxiras, Comput. Phys. **12**, 538 (1998).
[5] H. Rafii, L. Hua, and M. Cross, J. Phys.: Condens. Matter **10**, 2375 (1998).
[6] L. B. Freund, *Dynamical Fracture Mechanics* (Cambridge University Press, New York, 1990).
[7] E.G. Flekkøy, G. Wagner, and J.G. Feder, Europhys. Lett. **52**, 271 (2000).
[8] S.T. O'Connell and P.A. Thompson, Phys. Rev. E **52**, 5792 (1995).
[9] N.G. Hadjiconstantinou and A.T. Patera, Int. J. Mod. Phys. C **8**, 967 (1997).
[10] A.L. Garcia, J.B. Bell, W.Y. Crutchfield, and B.J. Alder, J. Comput. Phys. **154**, 134 (1999).
[11] M. Plapp and A. Karma, Phys. Rev. Lett. **84**, 1740 (2000).
[12] P.J. Hoogerbrugge and J.M.V.A. Koelman, Europhys. Lett. **19**, 155 (1992).
[13] P. Español, Phys. Rev. E **52**, 1734 (1995).
[14] E.G. Flekkøy and P.V. Coveney, Phys. Rev. Lett. **83**, 1775 (1999).
[15] E.G. Flekkøy, P.V. Coveney, and G. de Fabritiis, Phys. Rev. E **62**, 2140 (2000).
[16] M. Quarrie, *Statistical Mechanics* (Harper and Row, New York, 1976).
[17] J.P. Rivet, Complex Syst. **1**, 838 (1987).
[18] L. D. Landau and E. M. Lifshitz, *Fluid Mechanics* (Pergamon Press, New York, 1959).